Supplement Material

Sea Ice Fractures in a Warming World: Projected Changes in Leads and Ridges

Jan P. Gärtner[1], Thomas Jung[1], Xinyue Li[1], and Nils Hutter[2]

[1]Alfred-Wegener-Institut, Helmholtz Zentrum für Polar- und Meeresforschung, Bremerhaven, Germany

[2]GEOMAR, Helmholtz Zentrum für Ozeanforschung Kiel, Kiel, Germany

Methods - LKF Detection

The LKF detection algorithm (Hutter et al., 2019) identifies narrow regions of increased deformation within the deformation rate field. Since deformation rates along LKFs are influenced by the background deformation, a simple threshold applied to the deformation rate field is insufficient for accurate detection. Instead, edge detection techniques are required to identify regions where deformation rates that are significantly higher than the local background. To achieve this, a Difference of Gaussian (DoG) filter is applied. This filter subtracts a Gaussian-blurred version of the deformation map from a less blurred version of the same map. The resulting filtered image highlights areas of localized deformation, where pixels exceeding a predefined threshold d_{LKF} are marked as LKF pixels. After this detection of LKF pixels, a morphological thinning algorithm is used reduce the width of the LKFs to one pixel. These LKF pixels are then grouped into segments, with each segment representing contiguous marked pixels between intersections or the start and end points of individual LKFs. Next, the algorithm reconnects these segments based on thresholds for proximity, orientation, and deformation rate, ensuring that segments belonging to the same LKF are combined. During the tracking phase, detected LKFs in one time record are compared to their predicted positions in subsequent records, based on sea ice velocity fields. This step allows for consistent tracking of LKFs over time.

The LKF detection algorithm relies on several input parameters, most of which were set to their default values. The parameters modified for this study are listed in Tab. 1. The minimum and maximum radii of the DoG filter, the maximum elliptical distance and the minium LKF length are automatically scaled by the algorithm based on the spatial resolution of the input data. The DoG filtering threshold d_{LKF} has the most significant influence on

the detection process, as it determines which pixels are identified as LKF pixels. For this analysis, the threshold was set to $d_{LKF} = 0.01$ days^{-1}, the same value used in the SIREx study (Hutter et al., 2022), a model intercomparison project assessing the ability of different models to simulate LKFs. This value is sufficiently low to capture simulated LKFs while high enough to filter out noise in the deformation field. While the total number of detected LKFs is strongly dependent on the choice of d_{LKF}, the trend in LKF occurrence remains insensitive to changes in this parameter.

Parameter	Variable name	Value	Unit
DoG filtering threshold	dog_thres	0.01	days^{-1}
ice concentration threshold	aice_thresh	0.8	
temporal scaling coefficient	t_red	1	

Table 1: Parameters of the LKF detection algorithm modified from their default values.

Seasonal Cycle of LKFs

Both the total and mean length of LKFs exhibit substantial daily and interannual variability. To better illustrate their seasonal trends, the metrics were averaged over 10-year intervals. The mean values, along with their corresponding standard deviations, are shown for three representative decades across the simulation period.

As the sea ice cover weakens during the melting phase in May and June (Fig. **??**), the total length of LKFs increases (Fig. 1). However, as sea ice concentration continues to decline in July, the number of detected LKFs decreases due to the sea ice concentration threshold in the detection algorithm. Beginning in September, the increase in LKF occurrence aligns with the freezing phase and the associated increase in sea ice concentration, enabling more LKFs to be detected. From October onward, the total length of LKFs declines as the sea ice cover strengthens, leading to increased sea ice strength and reduced deformation and fracturing events.

During winter and spring, the total length of LKFs increases throughout the simulation time in periods where pack ice is present (Fig. **??**a). In summer and fall, it decreases from 2020 onward since although a sea ice cover remains during the summer months, sea ice concentration in most regions falls below the detection algorithm's threshold of 80 %. Consequently, the number of detected LKFs is significantly reduced in summer.

The mean length of LKFs reaches its maximum in Spring, continuously decreases during the melting phase until August, and increases from September on (Fig. 2). Throughout the simulation period, the mean LKF length consistently decreases across all months at a similar rate (Fig. **??**b).

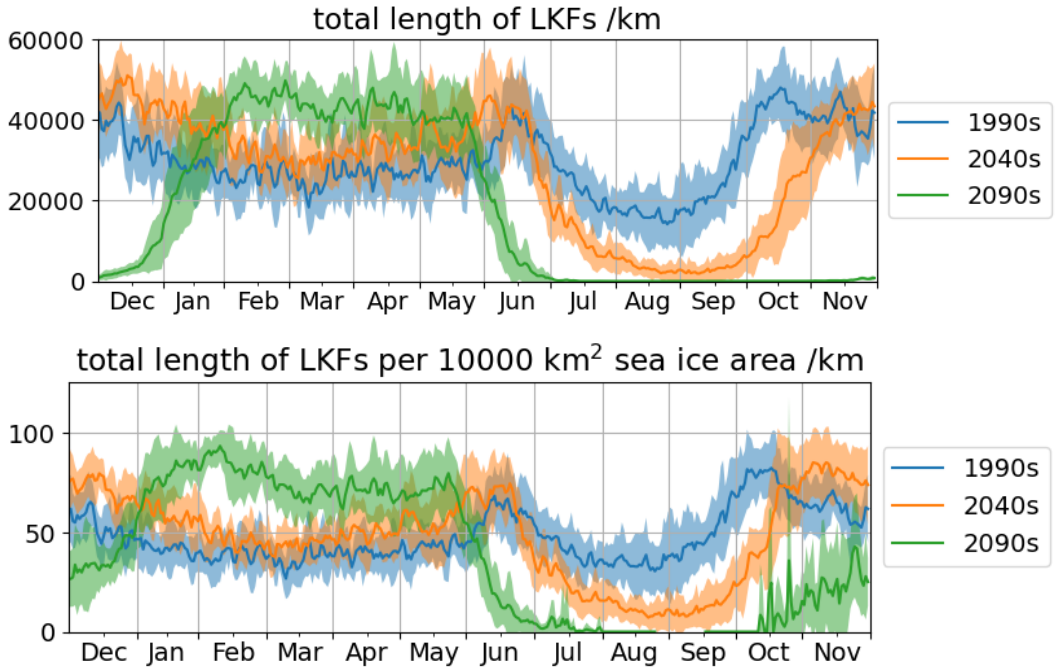

Figure 1: Seasonal cycle of the total length of LKFs and the total length of LKFs per sea ice area, averaged over 10-year intervals for three different time periods.

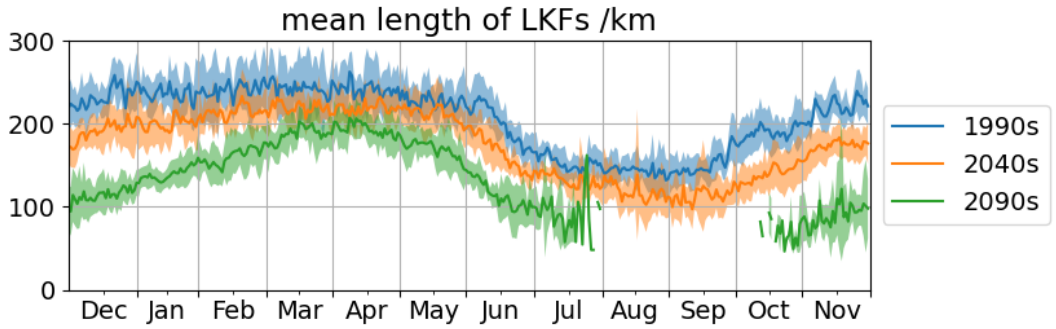

Figure 2: Seasonal cycle of the mean length of LKFs, averaged over 10-year intervals for three different time periods.

References

Hutter, N., Bouchat, A., Dupont, F., Dukhovskoy, D., Koldunov, N., Lee, Y. J., Lemieux, J.-F., Lique, C., Losch, M., Maslowski, W., et al. (2022). Sea ice rheology experiment (sirex): 2. evaluating linear kinematic features in high-resolution sea ice simulations. *Journal of Geophysical Research: Oceans*, 127(4):e2021JC017666.

Hutter, N., Zampieri, L., and Losch, M. (2019). Leads and Ridges in Arctic Sea Ice from RGPS Data and a New Tracking Algorithm. *The Cryosphere*, 13(2):627–645.